frontiers | Frontiers in Earth Science

TYPE Original Research
PUBLISHED 05 January 2023
DOI 10.3389/feart.2022.1077484

OPEN ACCESS

EDITED BY
Jian Liu,
Qingdao Institute of Marine Geology (QIMG), China

REVIEWED BY
Fangjian Xu,
Hainan University, China
Xiaozhong Huang,
Lanzhou University, China

*CORRESPONDENCE
Zhenke Zhang,
zhangzk@nju.edu.cn

SPECIALTY SECTION
This article was submitted to Quaternary Science, Geomorphology and Paleoenvironment, a section of the journal Frontiers in Earth Science

RECEIVED 23 October 2022
ACCEPTED 13 December 2022
PUBLISHED 05 January 2023

CITATION
Chen Y, Xia F, Zhang Z, Xu Q and Gui F (2023), Environmental and provenance change since MIS 2 recorded by two sediment cores in the central North Jiangsu Plain, East China.
Front. Earth Sci. 10:1077484.
doi: 10.3389/feart.2022.1077484

Environmental and provenance change since MIS 2 recorded by two sediment cores in the central North Jiangsu Plain, East China

Yingying Chen[1,2], Fei Xia[3], Zhenke Zhang[2]*, Qinmian Xu[4] and Feng Gui[5]

[1]School of Geography, Geomatics, and Planning, Jiangsu Normal University, Xuzhou, China, [2]The Key Laboratory of Coast and Island Development of Ministry of Education, School of Geography and Ocean Science, Nanjing University, Nanjing, China, [3]School of Geography, Jiangsu Second Normal University, Nanjing, China, [4]Tianjin Center, China Geological Survey, Tianjin, China, [5]Marine Science and Technology College, Zhejiang Ocean University, Zhoushan, China

In order to reveal the evolution of sediment provenance and paleoenvironment of the central North Jiangsu Plain (NJP) since marine isotope stage 2 (MIS 2), we analyzed lithology, accelerator mass spectrometry (AMS) ^{14}C dating, macrofossils and foraminifera, grain size, and geochemical compositions of sediments from two sediment cores (Core M and Core Y) recovered in the northern side of the Yangtze River. Our results show that fluvial environments prevailed in the central NJP during MIS 2, followed by alternations of coastal-marsh environments and shallow-bay environments in north central NJP and coastal-marsh environments in south central NJP during MIS 1. Provenance analysis suggests a major change in sediment provenance from the Yangtze River to the Yellow River at early MIS 1 in north central NJP; these Yellow River sediments might be transported from previously deposited sediments by strong tidal currents and intense waves to this area or be a reflection of a southward shift of the Yellow River during this period. However, the Yangtze River-derived sediments dominated the south central NJP since MIS 2. The depositional succession and sediment supplies since MIS 2 were dominantly controlled by sea-level fluctuations, regional geomorphic patterns, shift of the rivers, etc.

KEYWORDS

sedimentary environment, provenance, environmental evolution, Core Y, Core M, North Jiangsu Plain

1 Introduction

Coastal sedimentary records are important archives to understand the links between climate and sea levels. *In situ*-preserved sediments contain valuable information on marine–terrestrial interactions. Many studies have deciphered the sedimentary records from coastal areas worldwide to understand the history of relative sea-level changes (Hanebuth et al., 2000; Li et al., 2001; Shi et al., 2021), coastal stratigraphy, and environmental evolution on different spatial and temporal scales (Liu et al., 2016; Liu et al., 2018; Johnson et al., 2020; Zhou et al., 2021; Sun et al., 2022).

As a large sedimentary sink, the North Jiangsu Plain (NJP) is a key region connecting the land and ocean in the east of China, and it has preserved abundant environmental change information and provides a good medium for studying regional environmental change. In addition, the NJP is an important sediment reservoir for two globally large rivers: the Yellow River and the Yangtze

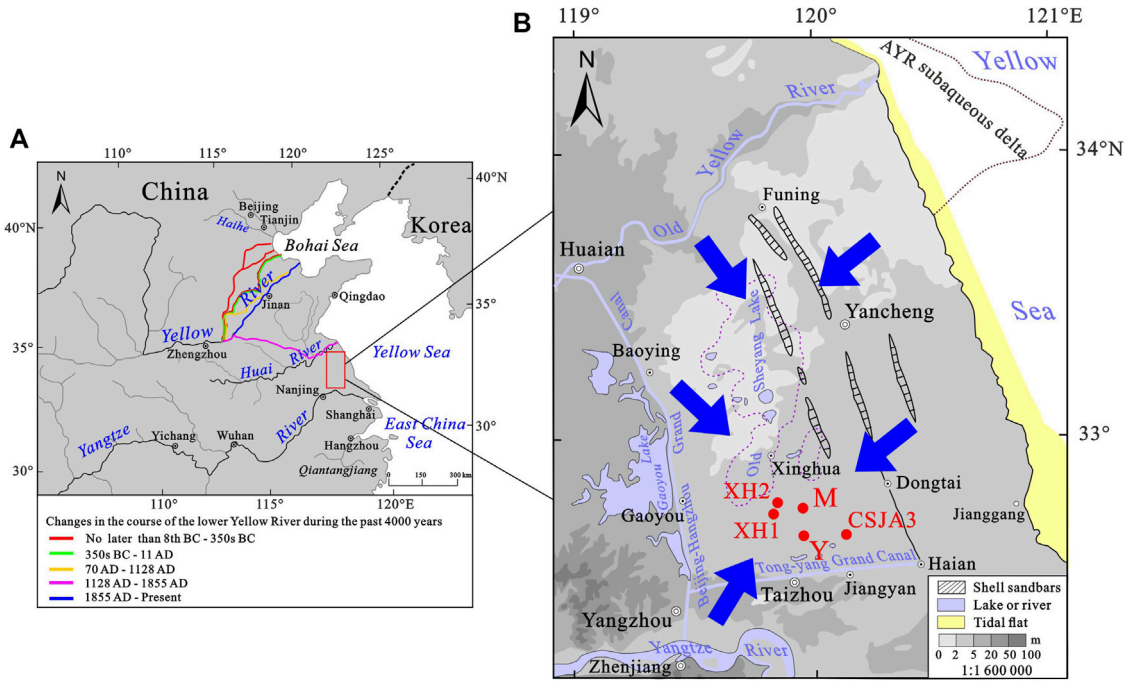

FIGURE 1
Left map **(A)** [modified after Yang et al. (2006)] showing the study area (the red rectangle area) and changes in the course of the lower Yellow River during the past 4000 years [Chen et al. (2012)]; right map **(B)** [modified after the Provincial Geomatics Center of Jiangsu Province (2004) and Gu et al. (1983)] showing the locations of the drill cores M and Y (M, Maoshan; Y, Yuduo), XH1 and XH2 (Zhang, 2009), and CSJA3 (Yu et al., 2016) in the northern part of the Yangtze River Delta; blue arrows denote the flow direction of possible sediment sources of the study area (AYR, Abandoned Yellow River).

(Changjiang) River. Therefore, sediments from the NJP will contain important paleoenvironmental information that is relevant to studying sea-level and tectonic variations, source-to-sink processes, etc. Great progress has been made in understanding the sedimentary evolution of the NJP since the Quaternary, especially over the Late Quaternary (e.g., Yang et al., 2002; Wang et al., 2006; Zhang, 2009; Zhang et al., 2010; Chen, 2016). Results have revealed that sedimentation in this region is characterized by the alternation of marine and terrestrial deposits. Comprehensive analyses of sediment cores from the central NJP reveal that sedimentary environmental changes since MIS 5 were strongly controlled by sea-level fluctuations, with most of the preserved sediments deposited in MIS 5, MIS 3, and MIS 1 (Chen, 2016). Using foraminifera abundances, one transgression layer has been identified in Core XH1 and Core XH2 (Figure 1B) (Zhang, 2009).

As the important sediment reservoir for the Yellow River and the Yangtze River, however, whether and to what extent the Yellow River and the Yangtze River supplied sediments to the central NJP is still controversial. Yang et al. (2002) noted that the Yangtze River had prevailed in the Jiangsu coastal plain sedimentation during the early stage of the Holocene, while the Yellow River dominated the area during the late Holocene. A study on the major, trace, and rare earth element characteristics of sediments in the Huaibei Plain demonstrated that the Yellow River may have migrated in the Huaihe River catchment during the last deglaciation (~13.2 ka) at least (Zhang et al., 2016). This result demonstrates that the influence of the Yellow River on the formation and shaping of the NJP may have been underestimated.

Given the complicated environment and provenance change, more case studies of sedimentary records from various locations around the NJP are needed, and investigations of high-resolution proxies of environmental changes will provide a better understanding of the sedimentary history in relation to the sea-level change. In this paper, two sediment cores (Core M and Core Y) with ~15 km apart in the northern side of the Yangtze River were obtained. Based on the lithology, AMS ^{14}C dating, grain size, and geochemical analyses of Core M and Core Y, changes in the sedimentary environment and provenance in the central NJP since MIS 2 were discussed. The results could provide important information for a better understanding of the formation and evolution of the NJP.

2 Study area

The central NJP is located between the Old Yellow River in the north and the Tongyang Grand Canal in the south (Figure 1). The topography of this area is dominated by lowland with a ground elevation below 5 m, and it declined from the Beijing–Hangzhou Grand Canal in the west toward the east along the Northern Jiangsu coast, with the lowest place around the Xinghua-Old Sheyang Lake area (Figure 1B). The Yangtze River and the Yellow River enter the East China Sea and the Bohai Sea, respectively. Although both rivers do not directly flow into the Yellow Sea at present, it was reported that they had frequently entered the Yellow Sea through the NJP during the Late Quaternary (Ren and Shi, 1986; Milliman et al., 1987; Chen and Stanley, 1995). For example, the deposition of huge amounts of sediment within the river channel and along the alluvial plain has caused frequent and extensive changes in the Yellow River's lower course (Figure 1A). The Yellow River shifted its river course from Shandong Province to the north Jiangsu coastal area in 1128 AD and delivered huge amounts of sediment to the coastal area and

TABLE 1 List of cores drilled from central NJP.

Core no.	Location		Elevation (m) (85 national datum)	Length (m)	Recovery (%)
	Latitude (°N)	Longitude (°E)			
M	32°45.051′	120°00.623′	~2	90	93.52
Y	32°38.713′	120°02.389′	~3	92	92.38

the Yellow Sea until 1855 AD; the coastline prograded rapidly, and the Abandoned Yellow River subaqueous delta was developed during this period (Ren and Shi, 1986; Milliman et al., 1987) (Figure 1). Following the capture in 1128–1855 AD by the Yellow River, the Huaihe River became a tributary of the Yellow River (Editorial Board on Records of Huaihe River, 1997). Abundant sediments supplied by the Yellow River also make the topography in the north NJP (near the Old Yellow River course) obviously higher than that in the south (Xinghua-Old Sheyang Lake area).

Sedimentary sequences of the Late Quaternary in the Jiangsu coastal plain and the northern Yangtze River Delta have been studied extensively on the basis of analysis of sediment cores (Li et al., 2001; Sun et al., 2015). The thickness of the Last Glacial Maximum (LGM) strata ranges from 2 m to 10 m, at a burial depth of 3–25 m, increasing eastward in burial depth and decreasing eastward in sedimentary thickness. This stiff clay layer was inferred to be compound ones resulting from alternating deposition and pedogenesis on the palaeo-interfluve of the Yangtze River, which became very hard after being exposed and dewatered (Li and Wang, 1998; Chen et al., 2008). At the end of the LGM, the topographic form in the area was tilted and uplifted from southeast to northwest, which significantly influenced the postglacial transgression (Chen et al., 1995). The paleo-coastline in the North Jiangsu Plain even reached the Huaiyin–Gaoyou–Yangzhou area (Pan, 1983), and a huge estuary of the Yangtze River with the apex at Zhenjiang and Yangzhou areas was formed when postglacial transgression reached the maximum (Li et al., 2000). After 7000 a BP, the sea level gradually tended to be stable, and this was evidenced by a series of shelly sandbars parallel to the present coastal line at the central part of the northern Jiangsu coastal plain area, which was developed at the Funing–Yancheng–Dongtai–Hai'an area with ~200 km long from north to south and ~60 km west of the present coastline (Figure 1B) (Gu et al., 1983).

3 Materials and methods

3.1 Core sampling

Two borehole cores (Core M and Core Y) were obtained in March 2014 from the back of the northern part of the Yangtze River Delta (Table 1; Figure 1). Core M and Core Y were split, descried, photographed, and subsampled in the laboratory immediately after the completion of drilling. In this study, we mainly focused on the upper 20 m of the whole core, where the age framework was effectively established by the AMS ^{14}C results.

3.2 Sediment grain-size analysis

Subsamples were generally taken at 10–50 cm intervals for grain-size analysis: intervals that, on visual inspection, appeared of relatively homogenous grain size were sampled less dense; intervals with more variations were sampled denser. A total of 75 and 46 samples were obtained from the upper 20 m of Core M and 10 m of Core Y, respectively. Each sample was 2 cm thick. The grain size was measured using a Malvern Mastersizer 2000 laser particle size analyzer. Before measuring grain size, samples were pretreated with 10% H_2O_2 and 0.1 N HCl to remove organic matter and biogenic carbonate, respectively. The results from the laser particle size analyzer were statistically processed using GRADISTAT software (Blott and Pye, 2001). The Folk and Ward (1957) classification scheme was adopted in this study. Analyses of grain size were carried out in the Key Laboratory of Coast and Island Development of the Ministry of Education, Nanjing University.

3.3 Elemental analysis

Bulk sediments were used in this study for chemical analysis. A measure of 0.1 g powdered samples of the sediment was digested with concentrated 1 ml HNO_3, 0.5 ml $HClO_4$, and 5 ml HF in a clean Teflon vessel at ~90°C for about 4 h until the digested solution was evaporated to dryness. Then, it was eluted with 1.5 ml aqua regia (3: 1 HCl: HNO_3) and 8.5 ml distilled water. Concentrations of major and trace elements were measured by ICP-AES (OPTIMA 5300DV, produced by PerkinElmer Company, United States of America). The contents of 17 elements (Al, Ca, Fe, K, Mg, Mn, Na, Ti, P, Ba, Cr, Cu, Li, Ni, Sr, V, and Zn) were tested. The detection limit was 0.00X-0. X mg/L, RSD≤2%. Chinese standard materials, GSS2 and GSS5, and several sandbank samples were analyzed with the sample sets in order to monitor the analytical precision and accuracy. The results show that relative deviations between measured and certified values are generally less than 10%, indicating satisfactory recoveries. Chemical analyses of all samples were carried out in the Center of Modern Analysis, Nanjing University.

3.4 Species identification of macrofossils and foraminifera

Four samples of macrofossils (i.e., bivalves and gastropods) were analyzed in the Nanjing Institute of Geology and Paleontology, Chinese Academy of Sciences. They were rinsed with clean water and dried thoroughly before being analyzed. Zheng (2013) and Zhang (2008) are the main references used in the species identification of macrofossils. Eight samples of foraminifera of Core M and five of Core Y were analyzed in the Marine Science and Technology College, Zhejiang Ocean University. Wang (1988) and Loeblich and Tappan (1988) are

TABLE 2 AMS ^{14}C dating results of Core M and Core Y.

Core	Sample no.	Depth (m)	Material	Measured ^{14}C age (a BP)	^{13}C/^{12}c (‰)	Conventional age (a BP)	Laboratory no.	Comment
M	M1	1.40	Organic-rich mud	5190 ± 30	−20.7	5260 ± 30	Beta-379364	Reliable
	M3	3.89	Shell	6050 ± 30	−3.8	6400 ± 30	Beta-379365	Reliable
	M12	7.28	Organic-rich mud	9870 ± 40	−21.3	9930 ± 40	Beta-379366	Reliable
	M4	12.33	Organic-rich mud	30,510 ± 160	−21.5	30,570 ± 160	Beta-379367	Reliable
	M8	19.88	Plant debris	NA	−28.6	>43,500	Beta-379368	Unreliable
Y	Y2	3.56	Shell	6150 ± 30	−8.5	6420 ± 30	Beta-379371	Reliable
	Y4	5.30	Organic-rich mud	15,320 ± 50	−22	15,370 ± 50	Beta-379372	Reliable
	Y6	8.33	Organic-rich mud	26,440 ± 110	−21.7	26,490 ± 110	Beta-379373	Reliable

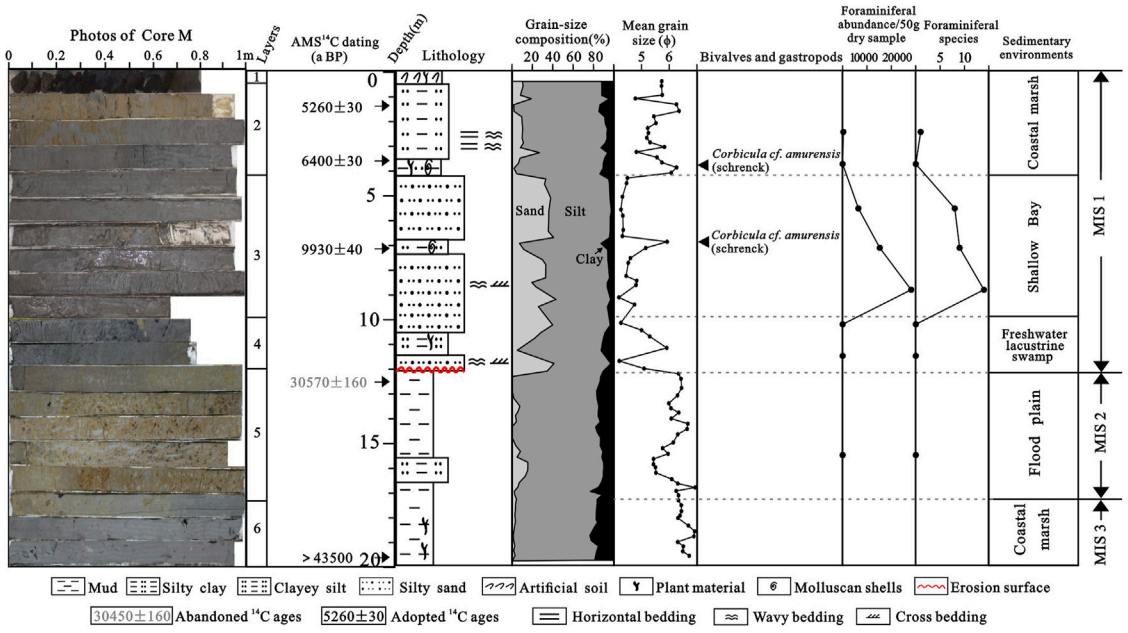

FIGURE 2
Comprehensive column of lithology, grain size, foraminiferal abundance, and species in Core M with AMS ^{14}C ages and interpreted sedimentary environments.

the main references used in the species identification of foraminifera.

3.5 AMS ^{14}C dating

Of the selected molluscan shells, plant debris, or organic-rich mud from these two cores, eight AMS ^{14}C ages were measured by Beta Analytic Inc. (Table 2). Age determinations were estimated based on a Libby half-life of 5568 years. To deal with the marine reservoir effect on the gastropod and shell samples, the ΔR value (135 ± 42) of a coastal sample from northwest Taiwan reported by Yoneda et al. (2007) was used.

4 Results

4.1 Sedimentary changes

Based on a comprehensive analysis of the testing results of Core M and Core Y, for example, sediment colors and components,

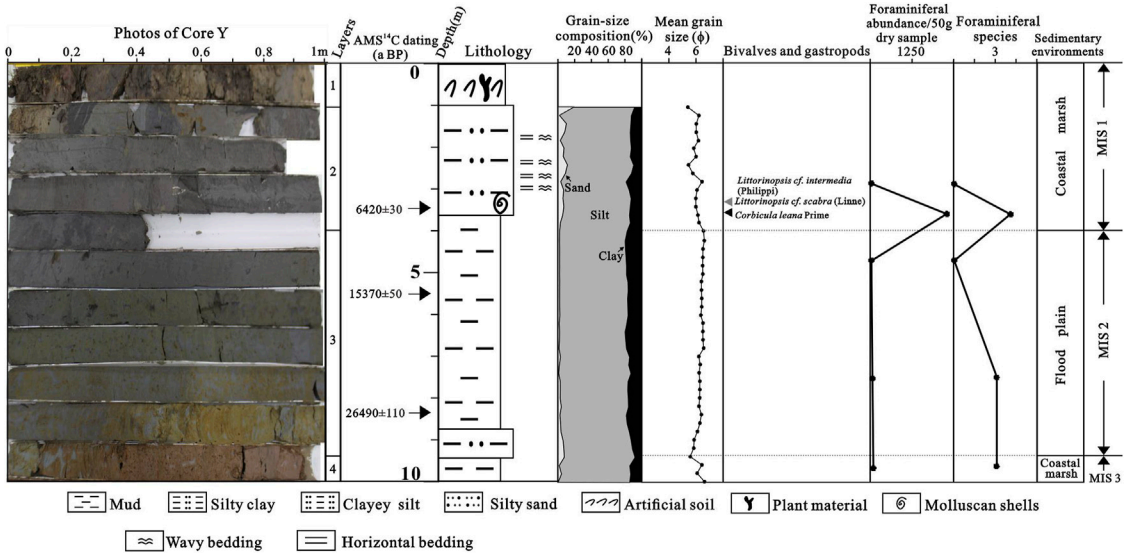

FIGURE 3
Comprehensive column of lithology, grain size, foraminiferal abundance, and species in Core Y with AMS ^{14}C ages and interpreted sedimentary environments.

sedimentary textures and structures, grain size, and macro- (i.e., bivalves and gastropods) and microfossils (i.e., foraminifer), the sediments in Core M and Core Y can be divided into five and three depositional units, respectively (Figure 2; Figure 3).

4.1.1 Sedimentary changes in Core M

Layer 5 (17.20–11.90 m): This layer is comprised of hardened or semi-hardened yellowish-brown stiff clayey silt, with abundant small black Fe-Mn nodules. The mean grain size is 5.09–6.93 ϕ, averaging 6.09 ϕ. No foraminifer was found in this layer. The contact relation between this layer and the underlying layer is transitional. This stiff mud layer is interpreted to be composed of river floodplain deposits that formed during MIS 2.

Layer 4 (11.90–9.94 m): Layer 4 is comprised of gray–black sandy silt with occasional wavy bedding, cross-bedding, and a few plant debris and mica pieces. The mean grain size ranges between 4.20 and 5.91ϕ, averaging 4.93ϕ. No foraminifer was found in this layer. The bottom contacts the underlying layer *via* an obvious erosion surface. Based on the aforementioned analyses, this section is interpreted as composed of freshwater lacustrine swamp deposits.

Layer 3 (9.94–4.10 m): Layer 3 is comprised of dark gray sandy silt, with occasional waving bedding, cross-bedding, and abundant mica pieces. A section of 6.71 m–7.00 m contained black mud, and plenty of intact or fragmentary shells were found. The mean grain size is 4.19–6.07ϕ, averaging 4.69ϕ. Foraminiferal abundances in this layer are extremely high, even reached to ~30,000/50 g dry sample, with 8–14 species. Within the foraminiferal assemblage, *Ammonia takanabensis* (Ishizaki) is the most abundant, followed by *Epistominella naraensis*, *Ammonia beccarii* (Linné) *var*, *Cribrononion vitreum*, *Astrononion tasmanensis*, *Brizalina striatula*, and *Florilus atlanticus*, all of them being the common benthic species in the present northern Jiangsu coastal area. Planktonic species *Globigerina* spp., which is both typical shallow marine and stenohaline species, was also identified in this layer, but all of them were young specimen fossils. All of the aforementioned foraminiferal species are attributed to the hyaline group. In addition, the porcelaneous group, with two specimens of *Quinqueloculina akneriana rotunda (Gerke)* and 12 specimens of *Quinqueloculina* spp, was observed in a sample at a burial depth of 8.85 m. Foraminiferal assemblage of benthic and planktonic species and euryhaline and stenohaline species, which are mixed with sandy silt, with high abundance and diversity, indicates that they might be transported by the tidal current for a long distance. *Corbicula cf. amurensis* (Schrenck), belonging to bivalves, was identified. The contact relation between this layer and the underlying layer is transitional. Based on the aforementioned analyses, this layer is interpreted as composed of shallow bay deposits.

Layer 2 (4.10–1.00 m): This layer is primarily comprised of gray–black and yellowish-brown clayey silt, with occasional wavy bedding and cross-bedding. At the bottom of the layer (3.45–4.00 m), plenty of plant debris, intact shells, and shell fragments were observed. The mean grain size ranges between 4.78 and 6.35ϕ, averaging 5.54ϕ. *Corbicula cf. amurensis* (Schrenck), belonging to bivalves, was identified, some of which had two valves hinged, indicating that they were *in situ* buried. Abundant foraminifera were observed in a sample at a burial depth of 2.45 m, but the foraminiferal assemblage is very monotonous; only *Ammonia beccarii* (Linné) var. was found. No foraminifer was found at 3.75 m. In addition, some of the foraminifers were etched and partially or wholly decalcified, presenting the antique white color. The contact relation between this layer and the underlying layer is transitional. This layer is interpreted as composed of coastal marsh deposits. Monotonous species and the one commonly dominating species of foraminifers are the most important characteristics of coastal marsh deposits (Wang et al., 1985). Results from Murray (1968) have shown that the diverse fields of hyposaline lagoons are very low, particularly for samples rich in silt and clay.

Layer 1 (1.00–0 m): This backfill soil layer is mainly comprised of gray–black and gray–yellow clayey silt, with a few rock dregs, plant roots, and debris.

4.1.2 Sedimentary changes in Core Y

Layer 3 (9.26–4.00 m): This layer is mainly comprised of hardened or semi-hardened yellowish-brown, olive green stiff clayey silt, with abundant small black Fe-Mn nodules. The mean grain size is 5.83–6.61ϕ, averaging 6.36ϕ. A total of 25, 4, and 2 specimens of *Quinqueloculina akneriana rotunda (Gerke)*, *Cribrononion vitreum*, and *Elphidium limpidum* were recognized in a sample at a burial depth of 7.53 m, respectively. The contact relation between this layer and the underlying layer is transitional. Based on the aforementioned analyses, this stiff mud layer is interpreted to be composed of river floodplain deposits that were formed during MIS 2. Foraminifers in this layer are very likely due to the reworking, transportation, and redeposition of sediments from the exposed marine strata, which were caused by paleo-storm during the LGM (Xia et al., 2013). Foraminifera are also found in the stiff clay mud of more than half of the sixteen cores, including cores T2, T4, T5, T6, T7, T9, T10, T13, and T15 (located in the Yangtze River Delta) (Chen et al., 2008). In addition, a few marine or estuarine shell fragments and calcareous nannofossils of core 07SR01 (located in the middle Jiangsu coast) and the marine shell fragment-mixed sand layers of core T9 were also found in the stiff muds (Zhao et al., 1997; Xia et al., 2013).

Layer 2 (4.10–1.00 m): This layer is primarily comprised of brownish-gray clayey silt, with occasional sand–mud thin layers. The mean grain size ranges between 5.40 and 6.45ϕ, averaging 5.98ϕ. At the bottom of the layer (3.3 m–3.7 m), plenty of intact shells and shell fragments were observed. *Littorinopsis cf. intermedia* (Philippi) and *Littorinopsis cf. scabra* (Linne), belonging to gastropods, were identified with one in each species, which usually inhabit near the high tide line. *Corbicula leana* Prime, belonging to bivalves, was present abundantly. Plenty of foraminifers were recognized at 3.64 m, and no foraminifer was found at 2.92 m in the core. The contact relation between this layer and the underlying layer is transitional. This layer is interpreted as coastal marsh deposits.

Layer 1 (1.00–0 m): This backfill soil layer is mainly comprised of gray–black and gray–yellow clayey silt, with a few rock dregs, plant roots, and debris.

4.2 Dating results

AMS ^{14}C dating results of Core M and Core Y indicated that the lower sections analyzed are older than 43,500 a BP and 26,490 ± 110 a BP (Table 2), respectively. Hence, they are considered to represent the Late Pleistocene.

4.3 Concentrations of major and trace elements in the core sediments

Elemental compositions of Core M and Core Y are given in Figure 4 and Figure 5. Major and trace elements show variable trends in concentrations of different depositional units of Core M (Table 3). Concentrations of most elements of sediments are generally higher in MIS 2 than in MIS 1 (Figure 4; Table 3). Except Na_2O and TiO_2, the rest of the elements all showed a decreasing trend (Figure 4), and concentrations of most elements (e.g., Al, Fe, K, Cr, Li, Ni, V, and Zn) are relatively close to the Yangtze River sediments (Table 3). Concentrations of most elements are slightly lower during MIS 1 but as a whole remain fairly stable; in spite of a sudden fluctuation at ~3.5 m, the average concentrations of most of the elements (e.g., Al, Fe, Mg, Ti, Cr, V, and Zn) are very close to the Yellow River sediments (Table 3).

Concentrations of most of the elements in sediments of Core Y show little variation since MIS 2 (Figure 5; Table 3), and the average concentrations of many elements (e.g., Fe, K, Ba, Cr, Ni, V, and Zn) are very similar to the Yangtze River sediments (Table 3).

5 Discussion

5.1 Chronostratigraphic framework

The establishment of a reliable chronostratigraphic framework is the foundation for studying and explaining many geological problems. Multiple layers of stiff clays, which are mottled dense argillaceous strata and easily distinguished due to their stiffness and abrupt contacts with overlying strata, have been found in the Late Quaternary sedimentary records of several major river deltas in the world, such as the Mississippi River Delta (Aslan and Autin, 1998) and the Yangtze River Delta (Li et al., 2002; Chen et al., 2008). For example, the first stiff clays that were found at depths of 3–28 m in the Yangtze River Delta possess a marked boundary with the overlying Holocene deposits and a diffuse boundary with underlying grayish-yellow littoral or fluvial silt and sandy clay (Chen et al., 2008). Therefore, the first stiff clays in the Yangtze Delta are useful and important regional markers in the stratigraphic framework of the eastern coastal areas of China. By using the AMS ^{14}C dating results, together with the first stiff clays for reference, a chronostratigraphic framework was established for the sedimentary succession of Core M and Core Y.

According to analyses of abundant ^{14}C dating results of a large number of drill cores in the Abandoned Yellow River Delta region of Jiangsu coastal plain, ^{14}C ages dated by organic carbon from clayey silt tend to be older owing to increased reworking and admixture of older carbon during transportation (Xia et al., 2015). Residues of the acid–alkali–acid extraction of the peaty layers and organic macrofossils such as larger wood fragments, *in situ* root remnants (Hanebuth et al., 2000), and shells (Xia et al., 2015) yielded the most reliable ages. For Core M, AMS ^{14}C age dated by plant debris from clayey silt at 19.88 m is >43,500 a BP, which could provide certain reference significance. AMS ^{14}C age dated by organic-rich mud from clayey silt at 12.33 m of Core M is 30,510 ± 160 a BP, which might be reliable. The material dated from the bottom of Layer 2 (3.89 m) was recognized as *in situ* buried marine shells that yielded an age of 6400 ± 30 a BP. AMS ^{14}C ages at 1.40 m and 7.28 m of peaty layers were also found to be reliable. For Core Y, AMS ^{14}C ages dated by organic carbon from clayey silt at the bottom (8.33 m) and the top (5.30 m) of Layer 3 are 15,370 ± 50 a BP and 26,490 ± 110 a BP, respectively. The material dated from the bottom of Layer 2 (3.56 m) was recognized as *in situ* buried marine shells that yielded a reliable age of 6420 ± 30 a BP.

Therefore, on the basis of the dates of global sea-level changes during the Late Quaternary (Waelbroeck et al., 2002), together with the AMS ^{14}C dates, and using the first stiff clays for reference, in Core M, Layer 6 (coastal marsh deposits), Layer 5 (floodplain deposits), Layer 4 (freshwater lacustrine swamp deposits), Layer 3 (shallow bay deposits), and Layers 2 and 1 (coastal marsh deposits) are interpreted to have been formed in the late MIS 3, MIS 2, early MIS 1, early to

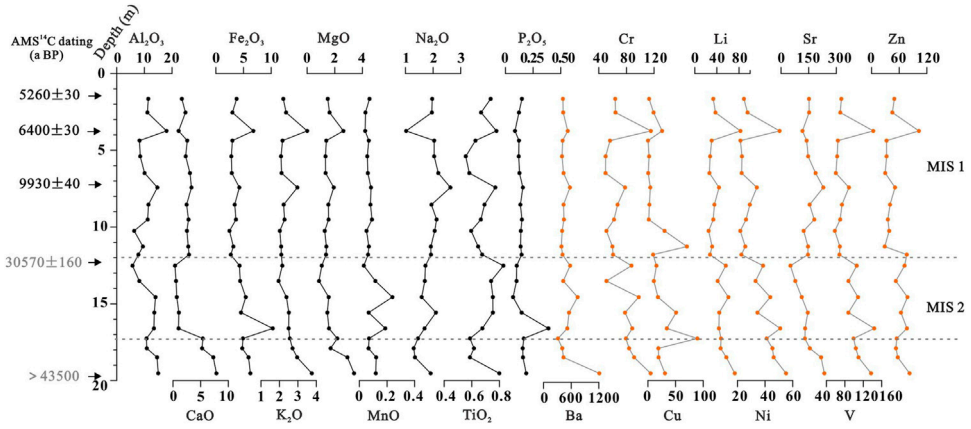

FIGURE 4
Elemental compositions of Core M sediments from the central North Jiangsu Plain (major elements in % and trace elements in μm/g).

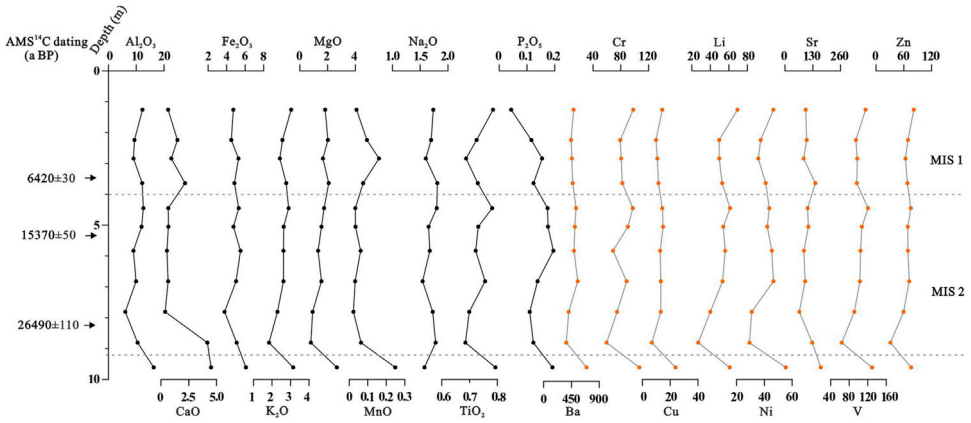

FIGURE 5
Elemental compositions of Core Y sediments from the central North Jiangsu Plain (major elements in % and trace elements in μm/g).

middle MIS 1, and middle-to-late MIS 1, respectively (Figure 2). In Core Y, Layer 4 (coastal marsh deposits), Layer 3 (floodplain deposits), and Layers 2 and 1 (coastal marsh deposits) are interpreted to have been formed in the late MIS 3, MIS 2, and middle-to-late MIS 1, respectively (Figure 3).

5.2 Evolution of sedimentary environments since MIS 2

The floodplain deposits suggest that in the area around the Core M and Core Y sites, a terrestrial environment prevailed during MIS 2. With the initiation of dramatic global cooling, the polar ice sheets advanced very quickly, and the sea level began to fall rapidly. The sea level of the Yellow Sea was situated at about −120 m during the LGM and later progressively rose to stabilize or slightly decrease at −100 m level and 16 cal ka BP (Figure 6) (Liu et al., 2004). Because of the extremely dry and cold climate during the LGM, a yellowish-brown-to/or-olive-green stiff clay mud was well developed in the northern side and southern side of the Yangtze River Delta with a buried depth of 3–25 m, which was the product of the ongoing accretion and pedogenesis on the floodplain during this period (Chen et al., 2008). This floodplain deposit was also well developed in the study area, and the stiff clay mud layer was recorded with a sedimentary thickness of 5.30 m in Core M and 5.26 m in Core Y. The burial depth in Core M and Core Y was 11.9–17.2 m (the depth of Core M and Core Y referred to in this study was the actual burial depth, not considering the compaction effect) and 4.0–9.3 m, respectively. As there was an erosion surface at the top of the MIS 2 deposit, the actual sedimentary thickness of this layer in Core M was certainly more than 5.3 m. The difference in sedimentary thickness of LGM deposits on the floodplain was a common phenomenon due to topographic fluctuations, distance from the river bed, and different water dynamic conditions in the Yangtze River Delta and the North Jiangsu Plain area (Chen et al., 2008).

The deglacial period began at ~15 cal ka BP as a result of global warming. The step-like and rapid rise of the postglacial sea level occurred as a result of global meltwater pulses (Figure 6) (Fairbanks, 1989; Liu et al., 2004). Freshwater lacustrine swamp, shallow bay, and coastal marsh deposits were developed in Core M during this period,

TABLE 3 Element concentrations in the sediments of Core M and Core Y (major element*: % and trace element: μm/g).

Element	Core M			Core Y			River	
	Mean	MIS 2-avg	MIS 1-avg	Mean	MIS 2-avg	MIS 1-avg	Yangtze	Yellow
Al_2O_3*	10.28	13.09	9.20	10.28	10.00	10.69	12.30	9.20
CaO*	1.91	2.97	1.51	1.23	1.18	1.31	4.00	4.61
Fe_2O_3*	3.75	4.80	3.35	4.88	4.90	4.84	5.50	3.14
K_2O*	2.27	2.53	2.16	2.57	2.48	2.70	2.21	1.94
MgO*	1.43	1.68	1.34	1.55	1.31	1.90	2.22	1.40
MnO*	0.07	0.09	0.06	0.06	0.04	0.09	0.11	0.06
Na_2O*	1.74	2.01	1.64	1.70	1.70	1.71	1.23	2.20
TiO_2*	0.66	0.73	0.63	0.73	0.73	0.73	0.92	0.60
P_2O_5*	0.13	0.15	0.12	0.14	0.15	0.11	0.15	0.14
Ba	474	562	440	470	474	464	512	540
Cr	70	81	66	82	80	85	82	60
Cu	17	26	13	12	13	12	35	13
Li	40	49	37	51	49	55	43	23
Ni	31	40	28	40	40	40	33	20
Sr	141	103	156	102	99	107	150	220
V	84	107	76	99	98	101	97	60
Zn	54	69	48	66	62	70	78	40

avg, average. The element compositions of the Yangtze River and Yellow River sediments are derived from Zhao and Yan (1992).

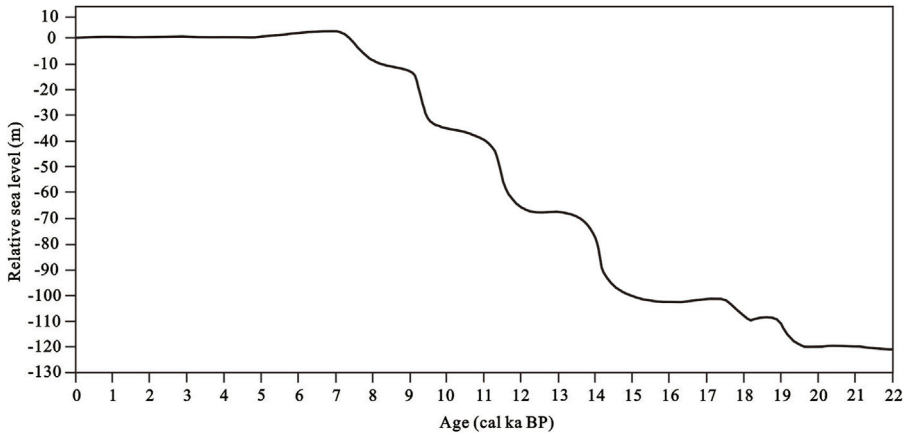

FIGURE 6
Stepwise postglacial sea-level rise in the western Pacific (after Liu et al., 2004).

and the corresponding grain size showed a coarse–coarse–fine pattern, indicating strong–strong–weak hydrodynamic conditions. The obvious erosion surface and sudden increase in grain size also demonstrated strong water dynamics during the postglacial period, which reflects that the top layer of the stiff clay mud formed during MIS 2 in Core M was eroded. Transgression layers with obvious erosion surfaces at the bottom were extensively distributed during the postglacial period in the continental shelves in eastern China (Li and Wang, 1998; Xia et al., 2013). The postglacial deposit thickness of Core Y is relatively small; only a 4 m coastal marsh deposit with fine grain size was developed, indicating relatively weak water dynamics.

Since the sea level reached a maximum at around 7000 a BP, the paleo-coastline at NJP even reached the Huaiyin–Gaoyou–Yangzhou area (Figure 1B), and a huge estuary of the Yangtze River with the apex

at Zhenjiang and Yangzhou areas was formed when the postglacial transgression reached the maximum (Li et al., 2000). After 7000 a BP, the sea level gradually tended to be stable (Figure 6); this was evidenced by a series of shelly sandbars (formed at ~7 ka BP, 4.6 ka BP, and 3.8 ka BP from west to east, respectively) parallel to the present coastline in the NJP, which have been found in Funing–Yancheng–Dongtai–Hai'an area (Figure 1B, Gu et al., 1983). These shelly sandbars, together with the north sandbank of the Yangtze River and the south sandbank of the Huaihe River, surrounded the central NJP, making this area a big shallow coastal lagoon that was separated from the open sea by shelly sandbars, which were linked with the open sea by a number of inlets (Pan, 1983). Core M and Core Y sites all developed coastal marsh deposits after 7000 a BP. Few foraminifer assemblages in Core M and Core Y during this period might be a reflection of a relatively long distance from the open sea or could be due to the etch of the calcareous shell at a low pH. Results from Murray (1968) have shown that the foraminifer assemblage in hyposaline lagoons diminishes sharply with the increasing distance to the open sea as salinity decreases from the back to the mouth.

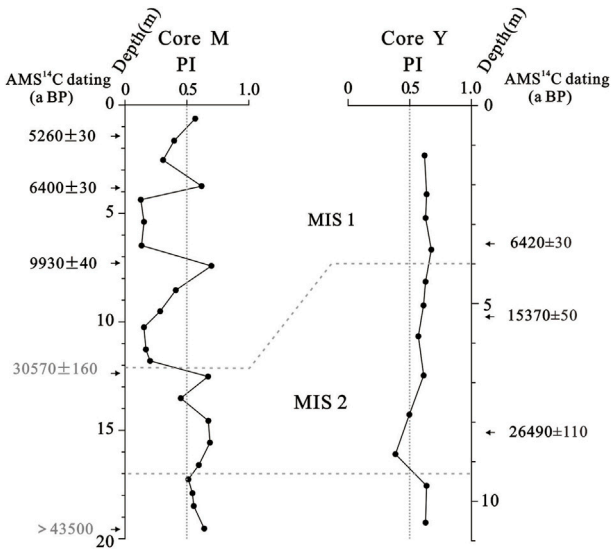

FIGURE 7
Depth profiles of PI values in Core M and Core Y.

5.3 Sediment provenance variation in the central NJP

5.3.1 Quantification of source contribution using the PI model

The sedimentation in the NJP is primarily controlled by large volumes of sediment derived from the surrounding large rivers (e.g., the Yangtze and Yellow rivers) and the smaller rivers (e.g., the Huai River). The modern Changjiang and Huanghe rivers, respectively, deliver 470 Mt and 1100 Mt of suspended sediments annually to the East Asian marginal seas (Milliman and Farnsworth, 2011). The contribution of other small localized rivers to the study area (e.g., the Huai River) is likely negligible because of the relatively low suspended sediment flux in total (e.g., ~14 Mt/yr of the Huai River) from these rivers (Milliman and Farnsworth, 2011). It has been well established that source rock compositions and weathering mechanisms basically impose constraints on the distinct geochemical compositions of the Yangtze River and the Yellow River sediments (Zhao and Yan, 1992; Chen et al., 2000; Yang et al., 2002). The Yangtze River sediments are characterized by high enrichment of transition metals (e.g., Cu, Zn, Pb, Fe, Co, Ni, Mn, Sc, and Ti), whereas the Yellow River sediments have relatively high concentrations of alkali and alkaline earth elements (e.g., Na, Ca, Sr, and Ba) (Zhao and Yan, 1992; Yang et al., 2002) (Table 3). Therefore, the marked difference in elemental compositions between both rivers' sediments could provide a basis for the discrimination of sediment sources in the North Jiangsu Plain. For the discrimination of the core sediments, five elements, namely, Al, Ti, Ni, Cr, and V, were chosen because these metals show big differences in concentrations between the Yangtze River and Yellow River and moreover, are known to behave conservatively in sedimentary environments (Taylor and McLennan, 1985; Yang et al., 2002). A two-end-member mixing model was adopted by assuming that the Yangtze River and the Yellow River are two provenances to the North Jiangsu Plain sediments and that the sediments from other sources (e.g., Huaihe River-derived sediments and sediments from other local small rivers, etc.; in fact, these rivers are too confined or too small to contribute much sediment) are negligible (Yu and Oldfield, 1989). This model has been applied in the modern Yellow River Delta (Yang et al., 2001), the north Jiangsu coastal plain (Yang et al., 2002), and west of the South Yellow Sea sediments (Lu, 2013) in China. A detailed computational process can be seen in Yang et al. (2002).

$$\mathrm{PI} = \frac{A_{i1}}{A_{i1} + A_{i2}},$$

$$A_{i1} = \sum_{i=1}^{n} \frac{|C_{ix} - C_{i1}|}{\mathrm{range}\,(i_{x,1})},$$

$$A_{i2} = \sum_{i=1}^{n} \frac{|C_{ix} - C_{i2}|}{\mathrm{range}\,(i_{x,2})},$$

where PI indicates provenance index; A_{i1} and A_{i2} represent degrees of similarity for element i of the sediment sample to the end-members 1 (Yellow River-derived sediment) and 2 (Yangtze River-derived sediment), respectively; C_{ix}, C_{i1}, and C_{i2} are concentrations of element i in the sediment sample and end-member sediments 1 and 2, respectively; the range is the difference between the maximum and minimum concentrations of element i in the sample and end-member sediments altogether; and n is the number of determined elements. Since the Yellow River and Yangtze River sediments are regarded as end-members 1 and 2, respectively, their theoretical PI values are expected to be 0 and 1, respectively. The whole composition of a sediment sample approximates that of end-member 1 if the PI nears 0, otherwise approximates that of end-member 2 if the PI approaches 1. Considering the bulk sample being used to determine element concentration in this paper, the values of Al, Ti, Ni, Cr, and V are derived from Zhao and Yan (1992).

Almost all of the PI values of the MIS 2 sediments of Core M are more than 0.50 with an average of 0.59 (Figure 7), implying that the sediments have been derived predominantly from the Yangtze River, whereas most of the PI values of the MIS 1 sediments are less than 0.50 (0.13–0.62) with an average of 0.32, representing a dominant influence from the Yellow River. Almost all of the PI values exceed 0.50 for the sediments of Core Y, averaging 0.59 (Figure 7); this indicated a

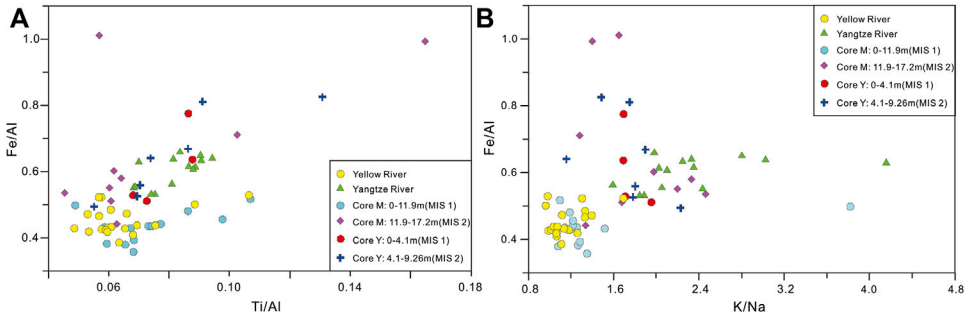

FIGURE 8
Cross plot of Fe/Al vs. Ti/Al **(A)** and Fe/Al vs. K/Na **(B)** of the M and Y core sediments from the NJP. Yellow River and Yangtze River element data are derived from Yang et al. (2002).

relatively stable sediment source from the Yangtze River for Core Y since MIS 2.

5.3.2 Sediment provenance discrimination using element ratios

The differences in elemental compositions between the Yangtze River and Yellow River sediments can be used as provenance indices to better understand the evolution and formation of the North Jiangsu Plain. Some element ratios, i.e., Fe/Al, K/Al, and Ti/Al, have especially been used to identify the sediment sources due to their relatively conservative behaviors during the sediment formation process (Han et al., 2019; Sun et al., 2019). K/Na is usually used as a proxy for the chemical maturity of sedimentary units. Chemical weathering is stronger in the Yangtze River basin than in the Yellow River basin, where physical weathering predominates (Yang et al., 2001). Therefore, the geochemical compositions of sediments derived from the Yangtze River and Yellow River can be distinguished based on the different weathering patterns and rock compositions (Yang et al., 2001). In this study, Fe/Al–Ti/Al and Fe/Al–K/Na scatter diagrams were used to identify the sources of sediments in the study area.

Figure 8 shows that the upper part (0–11.9 m) of the M core is clearly different from the lower unit (11.9–17.2 m) using plots of Fe/Al vs. Ti/Al and Fe/Al vs. K/Na, which indicates that the upper and deeper core units may have different provenances. The Fe/Al (0.36–0.52) and Ti/Al (0.05–0.11) values from 0 to 11.9 m in the M core fall within the ranges of the Yellow River field, implying that its source may be from the Yellow River. The Fe/Al (0.44–1.01) and Ti/Al (0.05–0.17) values of the lower part (11.9–17.2 m) are relatively widely distributed with some samples falling within the range of the Yellow River field and others seemingly falling within the range of the Yangtze River field (Figure 8). This implies that the source conditions of the deeper sediments are mainly composed of Yangtze and Yellow River sediments during MIS 2. Almost all samples of Core Y (0–4.10 m and 4.10–9.26 m) located in the Yangtze River field show very little variation and are unambiguously different from the Yellow River sediments (Figure 8); this trend can be interpreted to mean that the Y core sediments were primarily sourced from the Yangtze River.

Consequently, Fe/Al-Ti/Al and Fe/Al-K/Na ratios suggest that sediments settled on the study site during MIS 2 were mainly controlled by the Yangtze River, and later, Core Y in the southern part of NJP was dominated by Yangtze River sediments, whereas Core M in the northern part was supplied by the Yellow River for the last 10 ka.

5.4 Factors controlling environmental and provenance changes since MIS 2

Both PI values and Fe/Al-Ti/Al and Fe/Al-K/Na ratios indicate an alternating influence of the Yellow River and the Yangtze River on the North Jiangsu Plain since MIS 2. The Yangtze River sediments dominated the study area during MIS 2, and the MIS 1 sediments of Core Y still received the Yangtze River sediments, while Core M was controlled by the Yellow River-derived sediments.

The Yellow River-derived sediments in Core M were dark gray sandy silt and a large number of mica pieces were observed, indicating that these sediments might have been transformed and accumulated in this area by the transport of previously deposited sediments by strong tidal currents and intense waves during the transgression period. According to Chen (1989), sediments of the Yellow River usually show light yellow or yellow–brown color, which is composed of silt or silty sand, whereas once the sediments were transformed, the color would be darker because of the river–sea interaction. Waves and tides represent the dominant hydrodynamic forcing for the coast-shelf environment (Gao and Collins, 2014), especially in shallow waters, wave-generated currents can cause intense sediment transport (Dyer, 1986). The tidal current is often responsible for landward transport. Waves can cause landward transport of sand and gravel on the continental shelf (Gao and Collins, 2014), and the coarse grain size of PG sediments of Core M also indicates strong hydrodynamic conditions (Figure 2). Furthermore, the tidal current is also recognized as the primary agent of foraminifera transport, and the small size, high diversity, and stenohaline species of the foraminiferal assemblage are important marks of a strong-medium tidal estuary (Wang et al., 1986). The foraminiferal assemblage at 4.10 m–9.94 m in Core M is a mixture of benthic and planktonic species and euryhaline and stenohaline species, with high abundance and diversity, which might also be a reflection of strong tidal currents during this period.

Based on the lithologic characteristics of several cores, Chen (1989) concluded that the Yellow River sediments began to influence the North Jiangsu Plain in the Late Pleistocene. Liu et al. (1987) thought that the Yellow River might have directly flowed into the Yellow Sea in the northern Jiangsu coastal area for quite a long time during the Pleistocene. Zhang et al. (2016) proposed that the Yellow River invasion into the Huaihe River drainage basin occurred during the last deglaciation (~13.2 ka). In addition, on the basis of geochemical analysis, Yang et al. (2002) also detailed that the Yellow River supplied considerable

sediments to the north part of the Jiangsu coastal plain by tidal reworking or southward shift of the Yellow River during 7000–3000 a BP and somewhat to the central and southern parts. Some differences were observed when the Yellow River began to influence the North Jiangsu Plain since the postglacial period. These studies were primarily concentrated on the northern Jiangsu coast plain region, and the deposition rate of this area is usually not only higher but also strongly eroded; compiled with the late frequent scouring and redeposition, the stratigraphic sequence is extremely complex, which might disturb the proper understanding of the stratum development history (Li and Wang, 1998). However, the study area in this paper is located at the back of the northern part of the Yangtze River Delta and west of the northern Jiangsu coastal plain, with the relatively weak influence of the strong coastal hydrodynamic condition and physical and biological disturbances since the LGM, which might be a potential area for high-resolution stratigraphic study (Li and Wang, 1998). The results in this study clearly showed that the Yellow River supplied considerable sediments to part of the central North Jiangsu Plain during the postglacial period. The Yellow River probably had shifted its course to the south and may have directly flowed into the northern Jiangsu coastal area during the postglacial period. In addition, the Yellow River sediments might have accumulated in this area by the transport of previously deposited sediments by strong tidal currents and intense waves during the transgression period.

Although Core M and Core Y are only ~15 km apart, our research results show that the sedimentary environment and sediment source recorded by the two boreholes vary greatly. The burial depth of the MIS 2 deposit in Core M and Core Y was 11.9–17.2 m and 4.0–9.3 m, respectively. Therefore, the terrain of Core Y in the south of the study area is nearly 9 m higher than that of Core M in the north at late MIS 2. This topographic relief was an important factor controlling the direction and scope of transgression in the postglacial stage. Coupled with the climate change, sea-level fluctuation, and river channel migration of the Yangtze River, Yellow River, and Huaihe River in the historical period, the paleogeography and paleoenvironment evolution were extremely complex in the NJP; sediment stratigraphic records of the adjacent borehole even vary considerably, not only in the number of transgression layers but also in the lateral variation of sedimentary facies (Li and Wang, 1998). In fact, it is a common phenomenon in the Yangtze River Delta and the NJP area. For example, 3 and 4 transgression layers were recorded in Core M and Core Y since the middle Pleistocene, respectively (Chen, 2016). However, 1 transgression layer in XH1 and XH2 and 3 in CSJA3 were recorded since the Quaternary, respectively (Figure 1), which were only 10–20 km away from Core M (Zhang, 2009; Yu et al., 2016). A thorough review was carried out by Chen et al. (2020) on the distribution of buried channels in the region of NJP and the western South Yellow Sea; the results show that paleo-river channels are particularly developed in the region left behind by the paleo-Yangtze River since the Quaternary, resulting in a more complicated sedimentary environment and sediment source.

6 Conclusion

Based on a comprehensive analysis of Core M and Core Y, the evolution of the sedimentary environment and changes in sediment supplies of the central NJP were discussed.

River floodplain deposits were developed during MIS 2 in the central NJP. Coastal marsh deposits were developed in the south central NJP during MIS 1, and coastal marsh and shallow bay deposits were developed in the north central NJP during early MIS 1 when the postglacial transgression reached the maximum (~7000 a BP); after the postglacial transgression reached the maximum, the sea level tended to be stable, the paleo-coastline advanced to the east of the study area, and coastal marsh deposits were again developed in the north central NJP.

Sediments delivered to the study site during MIS 2 were mainly derived from the Yangtze River and were later dominated by the Yangtze River in the south and the Yellow River in the north. These Yellow River sediments might be transported from previously deposited sediments by strong tidal currents and intense waves to this area or be a reflection of a southward shift of the Yellow River during this period. Changes in sediment supplies and the sedimentary environment in the central NJP were controlled primarily by sea-level fluctuations, regional geomorphic patterns, and shift of the rivers.

Data availability statement

The original contributions presented in the study are included in the article/Supplementary Material; further inquiries can be directed to the corresponding author.

Author contributions

ZZ and YC designed the study; YC wrote the manuscript; YC, FX, and ZZ analyzed the data and contributed to the discussion and interpretation of the results; QX collated and processed the data; and YC and FG drew the drawings. All authors contributed to the article and approved the submitted version.

Funding

This work was supported by the National Natural Science Foundation of China (Grant Nos 41701101, 41901107, 41371024, and 41230751), the Open Fund of the State Key Laboratory of Loess and Quaternary Geology (Grant No. SKLLQ 1902), and a Project Funded by the Priority Academic Program Development of Jiangsu Higher Education Institutions.

Acknowledgments

The authors are very grateful to Prof. Xin Hu and Senior Engineer Yijun Chen at the Center of Modern Analysis, Nanjing University, for their assistance with the chemical experiment and to Huazhang Pan and Xiu Lan at the Nanjing Institute of Geology and Palaeontology, Chinese Academy of Sciences, for their assistance with the species identification of gastropod and bivalve fossils.

Conflict of interest

The authors declare that the research was conducted in the absence of any commercial or financial relationships that could be construed as a potential conflict of interest.

Publisher's note

References

Aslan, A., and Autin, W. J. (1998). Holocene flood-plain soil formation in the southern lower Mississippi valley: Implications for interpreting alluvial paleosols. *Geol. Soc. Am. Bull.* 110 (4), 433–449. doi:10.1130/0016-7606(1998)110<0433:HFPSFI>2.3.CO;2

Blott, S. J., and Pye, K. (2001). Gradistat: A grain size distribution and statistics package for the analysis of unconsolidated sediments. *Earth Surf. Proc. Land.* 26 (11), 1237–1248. doi:10.1002/esp.261

Chen, B. Z., Li, C. X., and Ye, Z. Z. (1995). Postglacial sedimentation and environmental evolution of the northern part of the Yangtze River Delta. *Acta Oceanol. Sin.* 17 (1), 64–75. (in Chinese).

Chen, J. S., Wang, F. Y., Li, X. D., and Song, J. J. (2000). Geographical variations of trace elements in sediments of the major rivers in eastern China. *Environ. Geol.* 39 (12), 1334–1340. doi:10.1007/s002540000224

Chen, Q. Q., Li, C. X., Li, P., Liu, B. Z., and Sun, H. P. (2008). Late quaternary palaeosols in the Yangtze delta, China, and their palaeoenvironmental implications. *Geomorphology* 100 (3), 465–483. doi:10.1016/j.geomorph.2008.01.015

Chen, X. X. (1989). Holocene sedimentary characteristics of the huanghuai plain, Jiangsu. *J. Stratigr.* 13 (3), 213–218. (in Chinese with English abstract).

Chen, Y. Y. (2016). *Evolution of depositional environment and sediment sources of the northern Yangtze River Delta since the middle Pleistocene*. Nanjing China: Doctor Dissertation of Nanjing University. (in Chinese with English abstract).

Chen, Y. Y., Xia, F., Zhang, Z. K., Xu, Q. M., and Chen, S. Y. (2020). Research progress on distribution of Quaternary buried paleo-Yangtze River channels in the North Jiangsu-Western South Yellow Sea. *Mar. Geol. Quat. Geol.* 40 (4), 40–54. (in Chinese with English abstract).

Chen, Y. Z., Syvitski, J. P. M., Gao, S., Overeem, I., and Kettner, A. J. (2012). Socio-economic impacts on flooding: A 4000-year history of the Yellow River, China. *Ambio* 41 (7), 682–698. doi:10.1007/s13280-012-0290-5

Chen, Z. Y., and Stanley, D. J. (1995). Quaternary subsidence and river channel migration in the Yangtze delta plain, eastern China. *J. Coast. Res.* 11 (3), 927–945.

Dyer, K. R. (1986). *Coastal and estuarine sediment dynamics*. Chichester: John Wiley.

Editorial Board on Records of Huaihe River (1997). *Annals of the Huaihe River* (Beijing: Science Press), 1. (in Chinese).*Records of Huaihe River*.

Fairbanks, R. G. (1989). A 17, 000-year glacio-eustatic sea level record: Influence of glacial melting rates on the younger dryas event and deep-ocean circulation. *Nature* 342 (6250), 637–642. doi:10.1038/342637a0

Folk, R. L., and Ward, W. C. (1957). Brazos River bar: A study in the significance of grain size parameters. *J. Sediment. Pet.* 27 (1), 3–26. doi:10.1306/74d70646-2b21-11d7-8648000102c1865d

Gao, S., and Collins, M. B. (2014). Holocene sedimentary systems on continental shelves. *Mar. Geol.* 352, 268–294. doi:10.1016/j.margeo.2014.03.021

Gu, J. Y., Yan, Q. S., and Yu, Z. Y. (1983). The cheniers of the northern coastal plain of Jiangsu Province. *Acta Sedimentol. Sin.* 1 (2), 47–59. (in Chinese with English abstract).

Han, L., Hao, Q. Z., Qiao, Y. S., Wang, L., Peng, S. Z., Li, N., et al. (2019). Geochemical evidence for provenance diversity of loess in southern China and its implications for glacial aridification of the northern subtropical region. *Quat. Sci. Rev.* 212, 149–163. doi:10.1016/j.quascirev.2019.04.002

Hanebuth, T., Stattegger, K., and Grootes, P. M. (2000). Rapid flooding of the sunda shelf: A late-glacial sea-level record. *Science* 288, 1033–1035. doi:10.1126/science.288.5468.1033

Johnson, S. Y., Beeson, J. W., Watt, J. T., Sliter, R. W., and Papesh, A. G. (2020). Controls on sediment distribution in the coastal zone of the central California transform continental margin, USA. *Mar. Geol.* 420, 106085. doi:10.1016/j.margeo.2019.106085

Li, C. X., Wang, P. X., Sun, H. P., Zhang, J. Q., Fan, D. D., and Deng, B. (2002). Late Quaternary incised-valley fill of the Yangtze delta (China): Its stratigraphic framework and evolution. *Sediment. Geol.* 152 (1), 133–158. doi:10.1016/S0037-0738(02)00066-0

Li, C. X., Chen, Q. Q., Zhang, J. Q., Yang, S. Y., and Fan, D. D. (2000). Stratigraphy and paleoenvironmental changes in the Yangtze delta during the late Quaternary. *J. Asian Earth Sci.* 18 (4), 453–469. doi:10.1016/S1367-9120(99)00078-4

Li, C. X., and Wang, P. X. (1998). *Late quaternary stratigraphy of the Changjiang delta*. Beijing: China Science Press. (in Chinese).

Li, C. X., Zhang, J. Q., and Deng, B. (2001). Holocene regression and the tidal radial sand ridge system formation in the Jiangsu coastal zone, east China. *Mar. Geol.* 173 (1), 97–120. doi:10.1016/s0025-3227(00)00169-9

Liu, J. P., Milliman, J. D., Gao, S., and Cheng, P. (2004). Holocene development of the Yellow River's subaqueous delta, north Yellow Sea. *Mar. Geol.* 209 (1), 45–67. doi:10.1016/j.margeo.2004.06.009

Liu, J., Wang, H., Wang, F. F., Qiu, J. D., Saito, Y., Lu, J. F., et al. (2016). Sedimentary evolution during the last ~1.9Ma near the western margin of the modern Bohai Sea. *Palaeogeogr. Palaeocl.* 451, 84–96. doi:10.1016/j.palaeo.2016.03.012

Liu, J., Zhang, X. H., Mei, X., Zhao, Q. H., Guo, X. W., Zhao, W. N., et al. (2018). The sedimentary succession of the last ~3.50 Myr in the western South Yellow sea: Paleoenvironmental and tectonic implications. *Mar. Geol.* 399, 47–65. doi:10.1016/j.margeo.2017.11.005

Liu, M. H., Wu, S. Y., and Wang, Y. J. (1987). *Late quaternary deposit of South Yellow Sea*. Beijing: China Ocean Press. (in Chinese).

Loeblich, A. R., and Tappan, H. (1988). *Foraminiferal genera and their classification*. New York: Van Nostrand Reinhold.

Lu, J. (2013). *Sedimentary characteristics and significance of provenance and sedimentary environment since the late Pleistocene in the western South Yellow Sea*. PhD Thesis (Institute of Oceanology, Chinese Academy of Sciences). (in Chinese with English abstract).

Milliman, J. D., and Farnsworth, K. L. (2011). *River discharge to the coastal ocean: A global synthesis*. New York: Cambridge University Press.

Milliman, J. D., Qin, Y. S., Ren, M. E., and Saito, Y. (1987). Man's influence on the erosion and transport of sediment by Asian rivers: The Yellow River (Huanghe) example. *J. Geol.* 95 (6), 751–762. doi:10.1086/629175

Murray, J. W. (1968). Living foraminifers of lagoons and estuaries. *Micropaleontology* 14 (4), 435–455. doi:10.2307/1485088

Pan, F. Y. (1983). A sketch of the transition of the lakes between the Yangtze River and the Huaihe in the late Holocene. *Sci. Geogr. Sin.* 3 (4), 361–368. (in Chinese with English abstract).

Provincial Geomatics Center of Jiangsu Province (2004). *Atlas of the Jiangsu Province*. Beijing: China Cartographic Publishing House. (in Chinese).

Ren, M. E., and Shi, Y. L. (1986). Sediment discharge of the Yellow River (China) and its effect on the sedimentation of the Bohai and the Yellow Sea. *Cont. Shelf Res.* 6 (6), 785–810. doi:10.1016/0278-4343(86)90037-3

Shi, X. F., Yao, Z. Q., Liu, J. X., Qiao, S. Q., Liu, Y. G., Li, X. Y., et al. (2021). Dominant role of sea level on the sedimentary environmental evolution in the Bohai and Yellow seas over the last 1 million years. *Front. Earth Sci.* 9, 638221. doi:10.3389/feart.2021.638221

Sun, S., Li, Y., Liu, D. W., and Hu, K. (2022). Clay mineralogical records in the North Bohai coast of China in the last century: Sediment provenance and morphological implications. *Front. Earth Sci.* 10, 865839. doi:10.3389/feart.2022.865839

Sun, X. Q., Liu, S. F., Li, J. R., Zhang, H., Zhu, A. M., Cao, P., et al. (2019). Major and trace element compositions of surface sediments from the lower bengal fan: Implications for provenance discrimination and sedimentary environment. *J. Asian Earth Sci.* 184, 104000–104010. doi:10.1016/j.jseaes.2019.104000

Sun, Z. Y., Li, G., and Yin, Y. (2015). The Yangtze River deposition in southern Yellow Sea during marine oxygen Isotope stage 3 and its implications for sea-level changes. *Quat. Res.* 83 (1), 204–215. doi:10.1016/j.yqres.2014.08.008

Taylor, S. R., and McLennan, S. M. (1985). *The continental crust: Its composition and evolution*. Oxford: Blackwell.

Waelbroeck, C., Labeyrie, L., Michel, E., Duplessya, J. C., McManusc, J. F., Lambeckd, K., et al. (2002). Sea-level and deep water temperature changes derived from benthic foraminifera isotopic records. *Quat. Sci. Rev.* 21 (1), 295–305. doi:10.1016/S0277-3791(01)00101-9

Wang, P. X. (1988). *Foraminifera and ostracod assemblage of bottom substrate of the East China Sea*. Beijing: China Ocean Press. (in Chinese).

Wang, P. X., Min, Q. B., and Bian, Y. H. (1985). Quaternary stratigraphy of marine-continental transitional facies in east China. *Quat. Sci.* 6 (1), 35–43. (in Chinese with English abstract).

Wang, P. X., Min, Q. B., and Bian, Y. H. (1986). Transport of foraminiferal tests in estuaries and its paleoenvironmental implications. *Mar. Geol. Quat. Geol.* 6 (2), 53–66. (in Chinese with English abstract).

Wang, Y., Zhang, Z. K., Zhu, D. K., Yang, J. H., Mao, L. J., and Li, S. H. (2006). River-sea interaction and the North Jiangsu Plain formation. *Quat. Sci.* 26 (3), 301–320. (in Chinese).

Xia, F., Zhang, Y. Z., Wang, Q., Yin, Y., Wegmann, K. W., and Liu, J. P. (2013). Evolution of sedimentary environments of the middle Jiangsu coast, South Yellow Sea since late MIS 3. *J. Geogr. Sci.* 23 (5), 883–914. doi:10.1007/s11442-013-1051-5

Xia, F., Zhang, Y. Z., Wang, R. F., Liu, J. P., Zhang, Z. K., and Peng, X. Q. (2015). Review for the studies on sedimentation range of the abandoned Yellow River subaqueous delta, North Jiangsu plain coast, China. *Acta Geogr. Sin.* 70 (1), 29–48. (in Chinese with English abstract).

Yang, S. Y., Cai, J. G., Li, C. X., and Deng, B. (2001). New discussion about the run-through time of the Yellow River. *Mar. Geol. Quat. Geol.* 21 (2), 15–20. (in Chinese with English abstract).

Yang, S. Y., Li, C. X., and Cai, J. G. (2006). Geochemical compositions of core sediments in eastern China: Implication for late Cenozoic palaeoenvironmental changes. *Palaeogeogr. Palaeocl.* 229 (4), 287–302. doi:10.1016/j.palaeo.2005.06.026

Yang, S. Y., Li, C. X., Jung, H. S., and Lee, H. J. (2002). Discrimination of geochemical compositions between the Changjiang and the Huanghe sediments and its application for the identification of sediment source in the Jiangsu coastal plain, China. *Mar. Geol.* 186 (3), 229–241. doi:10.1016/S0025-3227(02)00335-3

Yoneda, M., Uno, H., Shibata, Y., Suzuki, R., Kumamoto, Y., Yoshida, K., et al. (2007). Radiocarbon marine reservoir ages in the western pacific estimated by pre-bomb Molluscan shells. *Nucl. Instrum. Meth. B* 259 (1), 432–437. doi:10.1016/j.nimb.2007.01.184

Yu, J. J., Lao, J. X., Jiang, R., Zeng, J. W., Peng, B., Ma, X., et al. (2016). Reconstruction of the late quaternary palaeoenvironment on the north wing of Yangtze River Delta, based on comparative study of the multistratigraphies. *Geol. Bull. China* 35 (10), 1692–1704. (in Chinese with English abstract).

Yu, L. Z., and Oldfield, F. (1989). A multivariate mixing model for identifying sediment source from magnetic measurements. *Quat. Res.* 32 (2), 168–181. doi:10.1016/0033-5894(89)90073-2

Zhang, L., Qin, X. G., Liu, J. Q., Sun, C. Q., Mu, Y., Gao, J. L., et al. (2016). Geochemistry of sediments from the Huaibei Plain (east China): Implications for provenance, weathering, and invasion of the Yellow River into the Huaihe River. *J. Asian Earth Sci.* 121, 72–83. doi:10.1016/j.jseaes.2016.02.008

Zhang, M. H. (2009). Sedimentary infilling and environmental changes of the northern Jiangsu basin since latest Miocene recorded in Xinghua cores. Doctor Dissertation (Nanjing, China: Nanjing Normal University). (in Chinese with English abstract).

Zhang, S. P. (2008). *Atlas of marine molluscs in China*. Beijing: China Ocean Press. (in Chinese).

Zhang, Z. K., Xie, L., Zhang, Y. F., Xu, J., Li, S. H., and Wang, Y. (2010). Sedimentary records of the MIS 3 transgression event in the North Jiangsu plain, China. *Quat. Sci.* 30, 883–891. (in Chinese with English abstract).

Zhao, J., Li, C. X., and Zhang, G. J. (1997). Discovery of the tidal-genetic sandy sedimentary area at Subei coast plain and its geological significance. *J. Tongji Univ.* 25 (1), 82–86. (in Chinese).

Zhao, Y. Y., and Yan, M. C. (1992). Abundance of chemical elements in sediments from the Huanghe River, the Changjiang River and the continental shelf of China. *Chin. Sci. Bull.* 47 (15), 1201–1204. (in Chinese).

Zheng, X. D. (2013). *Atlas of aquatic molluscs in China*. Qingdao: Qingdao Publishing Group. (in Chinese).

Zhou, L., Shi, Y., Zhao, Y., Yang, Y., Jia, J., Gao, J., et al. (2021). Extreme floods of the Changjiang River over the past two millennia: Contributions of climate change and human activity. *Mar. Geol.* 433, 106418. doi:10.1016/j.margeo.2020.106418